Materials Research Proceedings **6** (2018) 125-130 doi: http://dx.doi.org/10.21741/9781945291890-20

Residual Stress Analysis in the Oxide Scales Formed on 316L Stainless Steel at 700 °C under Humid Air

LI Linwei[1,a], JI Vincent[1,b,*]

[1]ICMMO/SP2M UMR CNRS 8182, Université Paris-Sud, Bat. 410, 91405 Orsay Cédex, France

[a]linwei.li2@u-psud.fr, [b]vincent.ji@u-psud.fr

Keywords: Residual Stresses, High Temperature Oxidation, Water Vapor, X-Ray Diffraction

Abstract. The effects of water vapor on residual stresses in the oxide scales formed on 316L austenitic stainless steel are investigated. Samples were oxidized in thermogravimetric analyzer at 700°C for 6 hours - 96 hours with different amounts of water vapor (air, air+0.5%H_2O, air+4.0%H_2O). Grazing incidence X-ray diffraction (GIXRD) at different incident angles was used to study the phases and residual stresses in the oxide scales. The results demonstrate the formation of an inner chromia (Cr_2O_3) or chromium and iron solid solution ($Fe_xCr_{2-x}O_3$) layer and an outer hematite (Fe_2O_3), iron and nickel metallic compound ($FeNi_3$) and spinel layer. With the presence of water vapor, few wüstite (FeO) was also detected near the substrate. The residual stresses in the oxide scales are compressive, while the ones in the substrate are mostly tensile. Water vapor influenced not only the composition ratio of oxide scales and the residual stress levels but also the approach of oxide film damage.

Introduction

For austenitic stainless steels, which are widely used as constructional materials in power generation and petrochemical industries, a dense and continuous Cr-rich oxide film usually plays a protective role in the oxidation corrosion resistance at elevated temperature by acting as a barrier to prevent oxygen anion and metal cation inter-diffusion and reaction. However, these materials are meeting new challenges: higher working temperatures and more water vapor, among which the former is for gaining higher reaction efficiency and the latter is due to the more usage of biomass energy for environment cleanness [1]. For years many works concerning the high temperature oxidation mechanism of austenitic stainless steel have been reported [2-4], which intend that oxidation behaviors could be affected by various factors, such as the element composition in the substrate, the treatment of the substrate surface, the reactive gas, humidity and temperature. In addition, residual stresses which directly reflect the adhesion between the film and substrate are also taken attention [5]. The purpose of this work is to investigate the effects of water vapor on residual stress evolution in the Cr-containing oxide scale formed on 316L austenitic stainless steel at 700°C.

Experimental

A 316L stainless steel plant (the chemical composition is given in Table 1) was cut into a dimension 10×10×1mm with a 1mm in diameter hole drilled near the edge for being hung in the Thermal-gravimetric (TG) analyzer (SETARAM 92-16.18). Before oxidation, each side of samples were polished with SiC papers from P240 grit to P4000 grit to get a uniform surface roughness around 0.2μm, later immersed in the mixture solution of ethanol and acetone and kept in the ultrasonic cleaner for 10 minutes, then dried with pressed gas. TG experiments were carried out at 700°C from 6 hours to 96 hours in the air with different amounts of water vapor (dry air, air+0.5%H_2O and air+4.0% H_2O).

Content from this work may be used under the terms of the Creative Commons Attribution 3.0 license. Any further distribution of this work must maintain attribution to the author(s) and the title of the work, journal citation and DOI. Published under license by Materials Research Forum LLC.

Materials Research Proceedings **6** (2018) 125-130 doi: http://dx.doi.org/10.21741/9781945291890-20

After oxidation, the oxide scales were identified by GIXRD at incident angles of 0.5° and 2° respectively, using PANalytical X'Pert PRO MRD with copper radiation source (λ=0.154nm). Besides, Raman spectroscopy (λ=472.99nm) was also used to identify the chemical compositions of oxide sales as a reference. The microstructures of cross-section were studied by field emission gun scanning electron spectroscopy (FEG-SEM) equipped with an energy dispersive X-ray spectroscopy (EDX), using ZEISS SUPRA 55VP.

The residual stresses in both oxide scales and substrates were characterized by GIXRD, followed European standard NF EN 15305 (published in April 2009). The strongest peak of each phase was chosen (the {104} peaks for M2O3 and {111} peaks for substrate) in order to obtain sufficient intensities as well as positions of each peak at 13 distinct Psi angles (from -30° to +30°) were determined by using a Gauss function fitting.

Table 1 Chemical composition of 316L stainless steel (by weight %)

Fe	Cr	Ni	Mo	Mn	C	Si	P	S	N
Bal.	16-18	10-14	2-3	<2	<0.03	<0.75	<0.045	<0.03	<0.1

Oxidation product characterization

The 0.5° peak patterns of 316L stainless steel oxidized for 6 hours with different amounts of water vapor are presented in Fig. 1a, implying the generation of a corundum oxide M_2O_3 (M refers Cr, Fe or their solid solution) and an intermetallic compound ($FeNi_3$) during the initial oxidation. From Fig. 1b, the enlarged picture of Fig. 1a, it can been seen that the {104} peaks of Cr_2O_3 and Fe_2O_3 are overlapped under the condition of water vapor participation, while a more narrow peak without water vapor clears Cr and Fe solid solution phase ($Cr_xFe_{2-x}O_3$), because water vapor could accelerate the oxidation, promoting the stratification between Cr and Fe oxides from the beginning of reaction [6]. Fig. 1c shows the peak patterns obtained at different incident angles of 0.5° and 2° respectively after oxidation for 72 hours, suggesting the formation of few spinel structure oxides AB_2O_4 (A refers Mn or Fe, B refers Fe or Cr). Besides, wüstite (FeO) was detected near the substrate after oxidation in humid air, while spinel oxides preferred forming on the surface in dry air. In addition, the weight percent of M_2O_3 in the oxide scales were calculated by the software HighScore Plus and listed in Fig. 2.

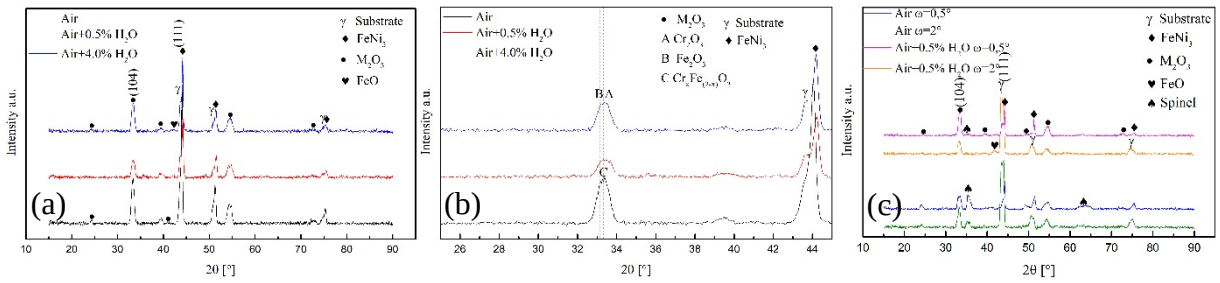

Fig. 1 GIXRD patterns of 316L stainless steel oxidized at 700°C with different amounts of water vapor (a) 6 hours, incident angle of 0.5° (b) enlarged figure of Fig. 1a (c) 72 hours, incident angles of 0.5° and 2°

Materials Research Proceedings **6** (2018) 125-130 doi: http://dx.doi.org/10.21741/9781945291890-20

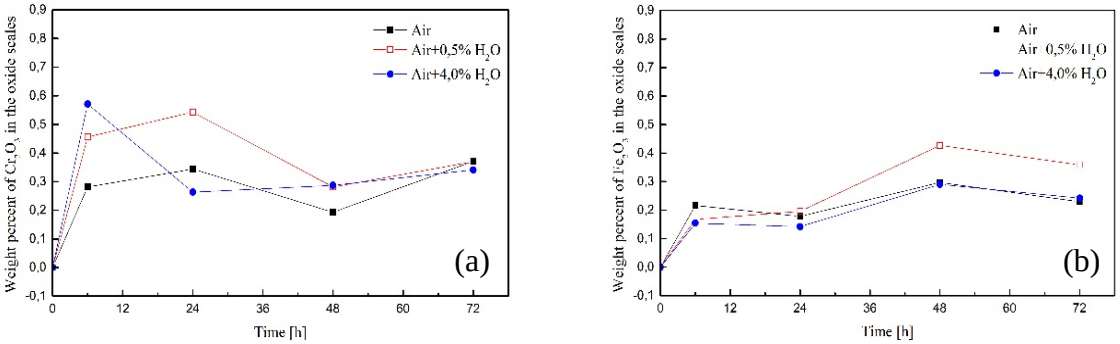

Fig. 2 Weight percent of each phase in the oxide scales by XRD semi-quantitative calculation (a) Cr_2O_3 (b) Fe_2O_3

Raman spectra depicts the evolution of oxidation products versus oxidation time under different moisture conditions, confirming the existence of Cr and Fe corundum oxide (Cr_2O_3, Fe_2O_3 or $Cr_xFe_{2-x}O_3$), demonstrated in Fig 3a-c. That a phenomenon matched with the XRD results can also be found. Cr-rich oxides grew within the first 24 hours but became replaced by Fe-rich oxides later, which means the protective Cr-rich oxide layer would lose their oxidation resistance properties gradually, and then lead to crack growth or delamination of oxide films [7]. Fig 4a gives the microstructure and element mapping of oxide scale after 200-hour oxidation in the dry air, revealing that the two-layer oxide scale is composed by the inner Cr-rich oxides and the outer Fe-rich oxides. Delamination happened along the interface between the two oxide layers and cracks generated through the outer layer. Fig. 4b describes the microstructure of oxide layer after 96-hour oxidation with 4.0% water vapor, in which wavy oxide layer formed and plenty of vacancies concentrated at the interface between the metal and oxide layer (O/M interface).

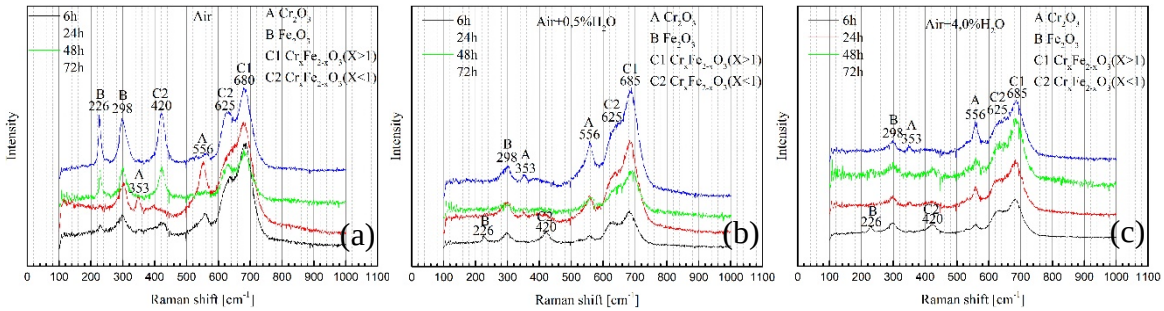

Fig. 3 Raman spectra of oxide scales formed at 700°C with different amounts of water vapor (a) air (b) air+0.5%H_2O (c) air+4.0%H_2O

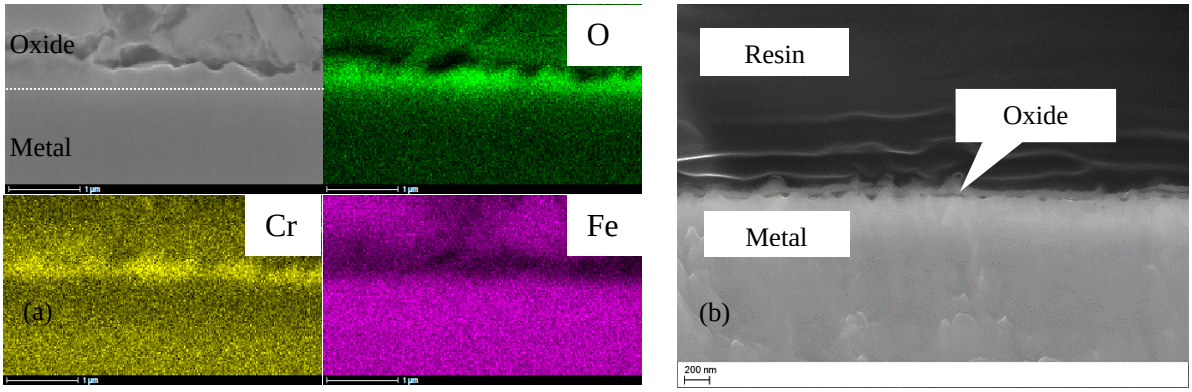

Fig. 4 SEM images and element mapping of oxide scales formed on 316L stainless steel at 700°C (a) 200-hour oxidation without water vapor (b) 96-hour oxidation with 4.0% water vapor

Materials Research Proceedings **6** (2018) 125-130 doi: http://dx.doi.org/10.21741/9781945291890-20

Residual stresses

The residual stresses in the oxide scales and substrate were studied by GIXRD technique at the incident angles of 0.5° and 2° respectively. The overlapping peaks of Cr_2O_3 and Fe_2O_3 were distinguished by profile fitting for all the patterns obtained at each Psi angle to determine the positions of each phase. The parameters needed for stress calculation were listed in Table 2 and the results are expressed in Fig. 5. It can be deduced from the fluctuating curves that the stress accumulation together with relaxation influenced the final values. The thermal stress produced during the cooling process makes contribution to the residual stresses simultaneously, which can be calculated according to Eq. 1.

$$\sigma_{\text{thermal}} = \frac{E_O(\alpha_O - \alpha_M)}{(1-\nu_O)}\Delta T, \quad (1)$$

where ΔT is the temperature difference, E is the Young's modulus, α is the thermal expansion coefficient and ν is the Poisson's ratio (O and M refer the oxide and metal respectively).

Fig. 5 The evolution of the residual stresses of the substrate and oxide scales (a) residual stresses in Cr_2O_3 (b) residual stresses in Fe_2O_3

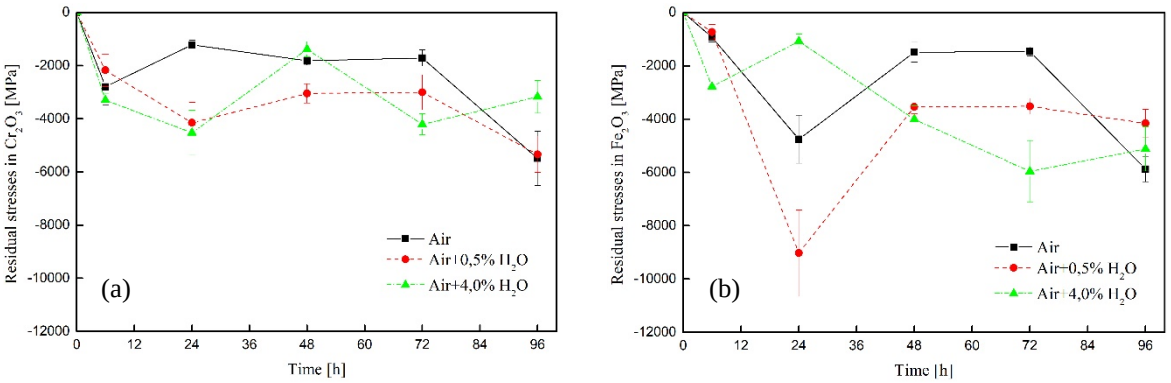

During the first 6 hours, the oxide layer formed in the dry air did not have a two-layer structure because of the diffusion rate limit, which is the same in the air with 0.5% H_2O. However, the oxide scale formed in the air with 4.0% H_2O contained much more Cr_2O_3 (≈57.1% in Fig. 2a), leading to stratification. So, the thermal stresses of Fe_2O_3 in those two cases are -734 MPa and +540 MPa, and of Cr_2O_3 are -2630MPa and -3410MPa respectively. Compared with the results in Fig. 5, it can be demonstrated that the residual stresses of Fe_2O_3 and Cr_2O_3 basically came from thermal stresses, except the one of Fe_2O_3 layer formed in the air with 4.0% water vapor, in which growth stress played an important role. That the residual stress of Cr_2O_3 formed in the air with 0.5% water vapor was less than the one formed in the dry air should be noticed, because the formation of FeO which has ability of deformation at high temperature could help relax partial stress [8].

Later but before 24 hours, the situations became more complicated. After oxidation for a while, the oxide scales had a two-layer distribution progressively, with a sharp rise of Cr_2O_3 (≈34.4% dry air, ≈54.3% 0.5% H_2O). There is a common agreement that Cr_2O_3 usually forms by Cr ion outward diffusion, which rarely causes stress except at the grain boundaries and defects [8]. In the dry air, the adhesion between Cr_2O_3 and the substrate was quite good after a long oxidation, illustrated in Fig. 4a. As a result, the residual stress of Cr_2O_3 formed in the dry air declined, which was affected by the deformation of the substrate at high temperature due to their compact

Materials Research Proceedings **6** (2018) 125-130 doi: http://dx.doi.org/10.21741/9781945291890-20

contact, indicating a tensile status during the oxidation. But in the humid air, vacancies preferred generating and gathering at the O/M interface, implying a bad adhesion [9]. So the residual stress of Cr_2O_3 formed in the humid air was less influenced by the substrate during the oxidation since the stress could relax through the pore formation. The residual stresses in Fe_2O_3 layer generated in the air with 4.0% H_2O shows an opposite trend compared with the other two cases, which is similar with Cr_2O_3 ratio (≈26.3%) in that condition. Due to the rapid consumption and diffusion of Cr, plenty of vacancies appeared at O/M interface and Cr depletion in the subscale of the substrate occurred [9], which reduced Cr_2O_3 and Fe_2O_3 to increase sustainably. Considering Cr-containing oxide usually has priority to generate, the residual stress of Fe_2O_3 decreased even though the residual stress accumulated in Cr_2O_3 layer.

Between 24 hours and 48 hours, cracking appeared in those three cases, but the fissure positions were different. For the condition of the dry air, the cracking preferred forming through the outer layer, which was displayed in Fig. 4a. The formation of the spinel oxides ($FeCr_2O_4$ or Fe_3O_4) above Cr_2O_3 was like an obstacle [10], impeding the anion and cation inter-diffusion, so that Fe_2O_3 generated continuously and the stress accumulated until cracking. The fissure was also situated in Fe_2O_3 layer in the air with 0.5% H_2O, because the residual stress of Fe_2O_3 decreased suddenly. However, for the condition of 4.0% water vapor, Cr_2O_3 layer was broken, which can be demonstrated by the new Cr_2O_3 formation (≈28.7%) and the decrease of residual stress of Cr_2O_3.

From 48 hours on, cracking or detachment continued happening, creating an unpredictable stress status. The competition of stress accumulation and relaxation were intense along with the new oxide generation, as well as fissure or delamination formation.

Table 2 Parameters for stress calculation

Phase	Young's modulus (E) [GPa]	Poisson's ratio (ν)	Thermal expansion coefficient (α) [10^{-6} K^{-1}]
Cr_2O_3	280	0.29	9.6
Fe_2O_3	220	0.19	12.5
Substrate	193	0.25	19.4

Summary

In conclusion, the oxide scales were characterized in this work, confirming the existence of a two-layer structure with an inner protective Cr-rich oxide and an outer non-protective Fe-rich oxide. The evolution of residual stress in the Cr_2O_3 layer was discussed, concerning the adherence between the oxide and substrate. During the incubation period, the residual stresses of Cr_2O_3 derived from the thermal stress during the cooling process for all the three conditions. After the two-layer structure formed, the residual stress of Cr_2O_3 began to be influenced by the growth stress simultaneously, which means that the outer layer may apply a compressed stress on it while the substrate may cause a contrast effect during the high temperature oxidation. Consequently, distinct oxidation conditions brought different results to the Cr_2O_3 layer. In the dry air, the Cr_2O_3 film kept compact and continuous, in which the spallation happened in the outer layer. Similarly, with few water vapor, the generation of vacancies could relieve stress to some extent, leading to an intact Cr_2O_3 film. However, with much more water vapor, the collective effects of pores at the O/M interface and the compressed loads from either the outer layer or the substrate contributed to the fold or damage generation in the Cr_2O_3 layer. For long oxidation, the competition of stress accumulation and relief excited the cracking or spalling in the oxide scale as well as the new oxide generation. It can be predicted that the oxidation resistance would lose rapidly in the case of more water vapor participation, and disastrous corrosion would happen in the case of dry air due to the replacement of Cr-rich oxide by Fe-rich

oxide. Less water vapor which could promote Cr_2O_3 formation and extend the exhausted time of Cr (reduce vacancies) may be a better choice.

References

[1] M. P. Brady, M. Fayek, J. R. Keiser, H. M. Meyer III, K. L. More, L. Anovitz, D. J. Wesolowski and D. R. Cole, Wet oxidation of stainless steels: New insights into hydrogen ingress, Corrosion Science. 53 (2011) 1633-1638. https://doi.org/10.1016/j.corsci.2011.02.011

[2] H. Falk-Windisch, J. E. Svensson and J. Froitzheim, The effect of temperature on chromium vaporization and oxide scale growth on interconnect steels for Solid Oxide Fuel Cells, Journal of Power Sources. 287 (2015) 25-35. https://doi.org/10.1016/j.jpowsour.2015.04.040

[3] X. Peng, J. Yan, Y. Zhou and F. Wang, Effect of grain refinement on the resistance of 304 stainless steel to breakaway oxidation in wet air, Acta Materialia. 53 (2005) 5079-5088. https://doi.org/10.1016/j.actamat.2005.07.019

[4] W. Kuang, X. Wu and E.-H. Han, The oxidation behaviour of 304 stainless steel in oxygenated high temperature water, Corrosion Science. 52 (2010) 4081-4087. https://doi.org/10.1016/j.corsci.2010.09.001

[5] J. Xiao, N. Prud'homme, N. Li and V. Ji, Influence of humidity on high temperature oxidation of Inconel 600 alloy: Oxide layers and residual stress study, Applied Surface Science. 284 (2013) 446-452. https://doi.org/10.1016/j.apsusc.2013.07.117

[6] C. Tedmon, The effect of oxide volatilization on the oxidation kinetics of Cr and Fe-Cr alloys, Journal of the Electrochemical Society. 113 (1966) 766-768. https://doi.org/10.1149/1.2424115

[7] M. Halvarsson, J. E. Tang, H. Asteman, J. E. Svensson and L. G. Johansson, Microstructural investigation of the breakdown of the protective oxide scale on a 304 steel in the presence of oxygen and water vapour at 600°C, Corrosion Science. 48 (2006) 2014-2035. https://doi.org/10.1016/j.corsci.2005.08.012

[8] T. Mitchell, D. Voss and E. Butler, The observation of stress effects during the high temperature oxidation of iron, Journal of Materials Science. 17 (1982) 1825-1833. https://doi.org/10.1007/BF00540812

[9] X. Wei, X. Peng, X. Wang and Z. Dong, Development of growth and thermal stresses in NiO scale on nanocrystalline Ni without and with dispersion of CeO2 nanoparticles, Corrosion Science. 118 (2017) 60-68. https://doi.org/10.1016/j.corsci.2017.01.014

[10] C. Fujii and R. Meussner, Oxide Structures Produced on Iron-Chromium Alloys by a Dissociative Mechanism, Journal of the Electrochemical Society. 110 (1963) 1195-1204. https://doi.org/10.1149/1.2425624